

Telomere shortening and chromosomal instability abrogates proliferation of adult but not embryonic neural stem cells

Sacri Ferrón^{1,*}, Helena Mira^{1,*†}, Sonia Franco^{2,*}, Marifé Cano-Jaimez¹, Elena Bellmunt¹, Carmen Ramírez¹, Isabel Fariñas^{1,‡} and María A. Blasco²

¹Departamento de Biología Celular, Universidad de Valencia, 46100 Burjassot, Spain

²Spanish National Cancer Center (CNIO), 28029 Madrid, Spain

*These authors contributed equally to this work

†Present address: Laboratory of Molecular Neurobiology, Department of Medical Biochemistry and Biophysics, Karolinska Institutet, 17177 Stockholm, Sweden

‡Author for correspondence (e-mail: isabel.farinass@uv.es)

Accepted 8 April 2004

Development 131, 4059-4070

Published by The Company of Biologists 2004

doi:10.1242/dev.01215

Summary

Chromosome integrity is essential for cell viability and, therefore, highly proliferative cell types require active telomere elongation mechanisms to grow indefinitely. Consistently, deletion of telomerase activity in a genetically modified mouse strain results in growth impairments in all highly proliferative cell populations analyzed so far. We show that telomere attrition dramatically impairs the *in vitro* proliferation of adult neural stem cells (NSCs) isolated from the subventricular zone (SVZ) of telomerase-deficient adult mice. Reduced proliferation of postnatal neurogenic progenitors was also observed *in vivo*, in the absence of exogenous mitogenic stimulation. Strikingly,

severe telomere erosion resulting in chromosomal abnormalities and nuclear accumulation of p53 did not affect the *in vitro* proliferative potential of embryonic NSCs. These results suggest that intrinsic differences exist between embryonic and adult neural progenitor cells in their response to telomere shortening, and that some populations of tissue-specific stem cells can bypass DNA damage check points.

Key words: Telomerase knockout, Neural progenitor, Neurogenesis, Differentiation

Introduction

Proliferation of neural stem cells (NSC)/neural progenitors largely determines the final size of neuronal populations during development and their subsequent renewal in postnatal neurogenic areas, but mechanisms regulating cycling of neural progenitors are poorly understood. NSCs are endowed with unlimited self-renewal capacity as well as multipotency to generate progeny that are fated to differentiate into the three major neural lineages (Reynolds and Weiss, 1992). They can be isolated from both the embryonic and mature mammalian CNS and expanded *ex vivo* under mitogenic stimulation for extended periods of time (reviewed by Gage, 2000; Temple, 2001). In the embryonic ventricular zone, NSCs are likely to coexist with fate-restricted progenitors all along the embryonic neuraxis (Temple, 2001). Stem-like cells from adult brains have been isolated not only from postnatal neurogenic regions, such as the hippocampus and the subventricular zone (SVZ), but from some non-neurogenic regions as well, including the spinal cord (see Gage, 2000). Thus, provided mammalian brains have residing cells with NSC properties in multiple locations, hope has been raised by the prospect of cell therapy based on reactivation of endogenous NSCs or on transplantation of *ex vivo*-expanded NSCs to replace neurons lost in traumatic or degenerative processes (Gage, 2000). The development of strategies to efficiently drive the differentiation and integration *in vivo* of these cells needs to be preceded by devising methods to obtain homogeneous, well characterized,

genetically stable populations of multipotential stem cells. Most studies aimed at understanding the nature of the signals involved in the regulation of NSC proliferation, self-renewal and differentiation have so far been concentrated on external signals, i.e. secreted growth factors, which induce NSCs to adopt specific decisions (see Johe et al., 1996; Gritti et al., 1996; Gritti et al., 1999; Tropepe et al., 1997; Taupin et al., 2000; Shimazaki et al., 2001; Lai et al., 2003). Fewer studies have addressed the role of intrinsic mechanisms in the regulation of NSC behavior (Groszer et al., 2001; Otshuka et al., 2001).

Telomeres are specialized chromatin structures at the ends of eukaryotic chromosomes that consist of non-coding single G-rich DNA repeats (TTAGGG in all vertebrates), bound to an array of associated proteins, and that play an essential role in chromosome capping (Greider, 1998; Blackburn, 2000). In most somatic tissues, telomeric DNA undergoes progressive shortening with each round of DNA replication, at a rate between 50 and 200 bp per cell division, resulting from incomplete replication of linear chromosomes by cellular DNA polymerases (see Blackburn, 2000). Telomere dysfunction, caused by significant loss of TTAGGG sequences or of telomere-binding proteins, leads to disruption of the telomere structure resulting in end-to-end chromosome fusions and genomic instability (de Lange, 2002). The non-homologous end-joining pathway for double strand break repair has been recently shown to mediate these outcomes of telomere

dysfunction, suggesting that a dysfunctional telomere is signaled as damaged DNA (Espejel et al., 2002a; Espejel et al., 2002b; Goytisolo and Blasco, 2002; Smogorzewska et al., 2002; d'Adda di Fagagna et al., 2003; Takai et al., 2003). Telomere shortening to a critical length, therefore, can activate DNA damage-induced pathways that trigger cell cycle arrest or apoptosis (Chiu and Harley, 1997; Goytisolo and Blasco, 2002). Thus, telomeric erosion limits the lifespan of dividing cells unless counteracted by elongation mechanisms, among which the best characterized is that mediated by the ribonucleoprotein telomerase. In telomerase-proficient cells, the reverse transcriptase component of the telomerase enzyme (*Tert*, telomerase reverse transcriptase) adds telomere repeat sequences to chromosome ends by using its RNA component (*Terc*, telomerase RNA component) as a template (Blackburn, 2000). Telomerase activation is an essential property of pluripotent embryonic stem cells and of some tissue-specific long-term self-renewing stem cells (Morrison et al., 1996; Thomson et al., 1998). In addition, high telomerase activity in germline cells, and telomerase activity upregulation in tumor cells and immortalized cell lines probably accounts for their unlimited lifespan (Kim et al., 1994; Chiu and Harley, 1997; Bodnar et al., 1998). Most somatic cells, however, express low or undetectable levels of telomerase activity resulting in progressive telomere attrition coupled to cell division (Harley et al., 1990; Prowse and Greider, 1995). The effects of telomere dynamics in vivo have been analyzed in mice that carry a deletion in the mouse telomerase RNA component and that, therefore, lack telomerase activity (Blasco et al., 1997). On a mixed C57BL6/129Sv (B6/Sv) genetic background these *Terc*^{-/-} mice are viable and fertile up to the fifth generation (G5) (Blasco et al., 1997; Lee et al., 1998; Herrera et al., 1999b). As telomeres shorten in *Terc*^{-/-} mice, at a rate of around 5 kb per generation, cytogenetic instability appears in multiple organ systems and results in decreased proliferation and increased apoptosis in highly proliferative tissues such as the reproductive and hematopoietic systems. Consistently, telomerase-deficient mice of late generations exhibit strain collapse due to increased infertility, reduced viability, and a wide spectrum of premature aging pathologies (Blasco et al., 1997; Lee et al., 1998; Rudolph et al., 1999; Herrera et al., 1999a; Herrera et al., 2000; Samper et al., 2002; Leri et al., 2003) (reviewed by Goytisolo and Blasco, 2002).

The role of telomerase and of telomere dynamics on neurogenic subsets, and in particular on NSC compartments, has not been addressed so far. High levels of both *Terc* and *Tert* mRNA are present in the developing neural tube as early as E10.5 (Martín-Rivera et al., 1998; Herrera et al., 1999b). Later, both *Terc* and the *Tert* mRNA are found in different regions of the developing murine CNS, in a complex pattern of gene expression characterized by a temporal correlation with proliferation of neural progenitors in different areas (Prowse and Greider, 1995; Greenberg et al., 1998; Martín-Rivera et al., 1998; Fu et al., 2000; Haik et al., 2000; Ostefeld et al., 2000; Klapper et al., 2001). These expression patterns suggest a role for telomerase in neural precursor biology. More recently, telomerase activity has also been demonstrated in neural precursor cells isolated from the adult SVZ and hippocampus (Caporaso et al., 2003). By comparison with other stem cell populations, the current working model holds that expression

and activity of telomerase in actively cycling neural progenitors may overcome the progressive proliferation-induced telomere shortening and promote growth and survival of progenitors.

We have analyzed neural progenitor proliferation in embryos and adult telomerase-deficient mice with shortened telomeres. We have found that cell proliferation is severely impaired in the SVZ of late-generation telomerase-deficient mice and that NSCs isolated from this region are not capable of in vitro expansion under mitogenic stimulation (see also Wong et al., 2003). Surprisingly, NSCs from late-generation telomerase-deficient embryos proliferated normally despite having shortened telomeres, cytogenetic abnormalities and increased levels of nuclear p53. Altogether, these findings reveal a fundamentally different response to telomere dysfunction and p53 activation in embryonic versus adult NSCs.

Materials and methods

In vivo analysis

Wild-type or *Terc*-deficient mice of the second (G2) and fourth (G4) generation in a mixed C57BL6/129Sv genetic background (Blasco et al., 1997) were perfused with 4% paraformaldehyde (PFA) in 0.1 M phosphate buffer, pH 7.4 (PB). After overnight postfixation, the brains were removed from the skull, washed in PB for 2 hours, dehydrated and embedded in paraffin wax. Embryos were fixed in Carnoy's fixative and processed as previously described (Fariñas et al., 1996). For BrdU labeling of proliferating cells in the adult brain, mice received seven intraperitoneal (i.p.) injections of 50 µg/g body weight BrdU every 2 hours and were killed 1 hour after the last one. The injection protocol for embryonic precursor labeling consisted in a single i.p. injection to pregnant mothers at the appropriate gestation times 1 hour before sacrifice. Methods for immunocytochemistry, for Nissl staining and for TUNEL labeling on paraffin sections, as well as methods for quantitative analysis in sensory ganglia, have been described previously (Fariñas et al., 1996). Primary antibodies used were: anti-GFAP (Dako), anti-BrdU (Dako), anti-PSA-NCAM (Chemicon), anti-NF 150 kDa (Chemicon). To determine the volumes of the olfactory bulbs and striatum, area measurements of these structures were obtained using Visilog[®] software every seven sections in complete series of coronal sections containing the portion of the olfactory bulb between the accessory olfactory bulb and the olfactory ventricle (see schematic drawing in Fig. 1) or the complete striatum.

NSC cultures

Adult 3- to 4-month-old pregnant and non-pregnant C57BL6/129Sv G4 *Terc*^{-/-} and wild-type female mice were killed by cervical dislocation. To initiate each independent culture, the brains of two different animals were dissected out and the regions containing the SVZ were isolated from each hemisphere and washed in Earle's balanced salt solution (EBSS; Gibco). Tissues were transferred to EBSS containing 1.0 mg/ml papain (Worthington DBA), 0.2 mg/ml L-cystein (Sigma), 0.2 mg/ml EDTA (Sigma) and incubated for 30-60 minutes at 37°C. Tissue was then rinsed in EBSS for 10 minutes, transferred to Dulbecco's modified Eagle's medium (DMEM)/F12 medium (1:1 v/v; Life Technologies, Gaithersburg, MD, USA) containing 0.7 mg/ml ovomucoid (Sigma), and carefully triturated with a fire-polished Pasteur pipette to a single cell suspension. To initiate each independent embryonic culture, the ganglionic eminences of three different embryos at gestational day 14.5 (E14.5; morning of the vaginal plug was taken as day 0.5) were dissected out, and mechanically dissociated. Isolated cells were collected by centrifugation, resuspended in DMEM/F12 medium containing 2 mM L-glutamine, 0.6% glucose, 9.6 g/ml putrescine, 6.3 ng/ml progesterone, 5.2 ng/ml sodium selenite, 0.025 µg/ml insulin, 0.1

mg/ml transferrin, 2 μ g/ml heparin (sodium salt, grade II; Sigma) (control medium) and supplemented with EGF and FGF2 (human recombinant, 10 and 20 ng/ml respectively; Peprotech, Rocky Hill, NJ, USA) (complete medium), and plated at 3000 cells/ml into 35 mm plastic dishes. For each passage, spheres formed after 4–6 days in vitro (DIV; embryonic NSC cultures) or 6–10 DIV (adult NSC cultures) were mechanically dissociated into a single-cell suspension and replated in complete medium. The total number of viable cells was determined at each passage by Trypan Blue exclusion. For cell growth assessment, a fraction of the culture at any given passage point, consisting in 250,000 viable cells, was plated and the number of cells generated was determined at the time of the next passage. To generate the accumulated cell growth curves, the ratio of cell production at each subculturing step was multiplied by the number of cells at the previous point of the curve. This procedure was repeated for each passage. For BrdU incorporation analysis, suspensions of dissociated cells at a density of 25000 cell/ml were cultured for 24 hours in complete medium with 2 μ M BrdU and the spheres formed were seeded onto poly-L-lysine-coated glass coverslips, fixed with 4% paraformaldehyde in PB for 20 minutes and rinsed three times in PB. For BrdU detection, the coverslips were then treated with 2 N HCl for 15 minutes, neutralized in 0.1 M borate buffer (pH 8.5), and incubated for 90 minutes at 37°C with mouse anti-BrdU antibodies (1:250; Dako) in PB containing 10% normal goat serum (NGS) and 0.3% Triton X-100 (blocking buffer). Following several washes, spheres were incubated with Cy3-conjugated anti-mouse antibodies (Jackson ImmunoResearch Laboratories Inc., West Grove, PA, USA) at 1:2000 dilution in blocking buffer for 45 minutes, rinsed several times in PB, counterstained with DAPI and mounted with Fluorosave (Calbiochem, La Jolla, CA). The percentage of cells that were BrdU-positive were determined for each group by counting the number of labeled and unlabeled cells. For p53 immunostaining, neurospheres were grown for several days and subsequently seeded onto poly-L-lysine-coated glass coverslips, fixed in cold acetone-methanol and immunofluorescence was performed as described using as a primary antibody a mouse anti-p53 (Oncogene) at a 1:100 dilution and a Cy5-conjugated secondary antibody at a 1:2000 dilution.

Measurement of telomere lengths and cytogenetic analysis

For quantitative fluorescence in situ hybridization (Q-FISH) analysis, cultured cells were incubated in hypotonic buffer (0.56% KCl) for 5 minutes at room temperature, fixed in methanol:acetic acid (3:1) and dropped onto wet slides. After drying overnight, cells were fixed in formaldehyde, digested with pepsin (1 mg/ml), dehydrated through graded ethanol and incubated with a fluorescent telomeric peptic nucleic acid probe (Cy3-(AATCCC)₃), as described previously (Blasco et al., 1997). After washing, cells were dehydrated and mounted in Vectashield with DAPI (Vector Laboratories, Burlingame, CA, USA). Images were captured using a Leica microscope LEITZ DMRB equipped with a 100 \times /NA 1.0 objective lens and a COHU High Performance CCD camera, with a red fluorescence filter (Leica I3-513808) for the Cy3-conjugated telomeric probe and a DAPI fluorescence filter (Leica A-513808) for the nuclear imaging. For metaphase analysis, 10 metaphases per sample were analyzed using Leica Q-FISH v2.1 software. Fluorescence beads (Molecular Probes, Eugene, OR, USA) were used as quantification standards, as described previously (Hande et al., 1999). For interphase cells, 50 interphase nuclei were captured. To translate arbitrary fluorescence units to kb, two murine lymphoma cell lines of known telomere length (length ratio, 7:1) were assayed in parallel and used to generate a linear regression curve (McIlrath et al., 2001). After Q-FISH hybridization, 50 metaphases were captured at 100 \times magnification and evaluated for cytogenetic abnormalities, such as aneuploidy and fusions. Chromosomes lacking telomeres were identified and counted from 10 metaphases using Leica Q-FISH software.

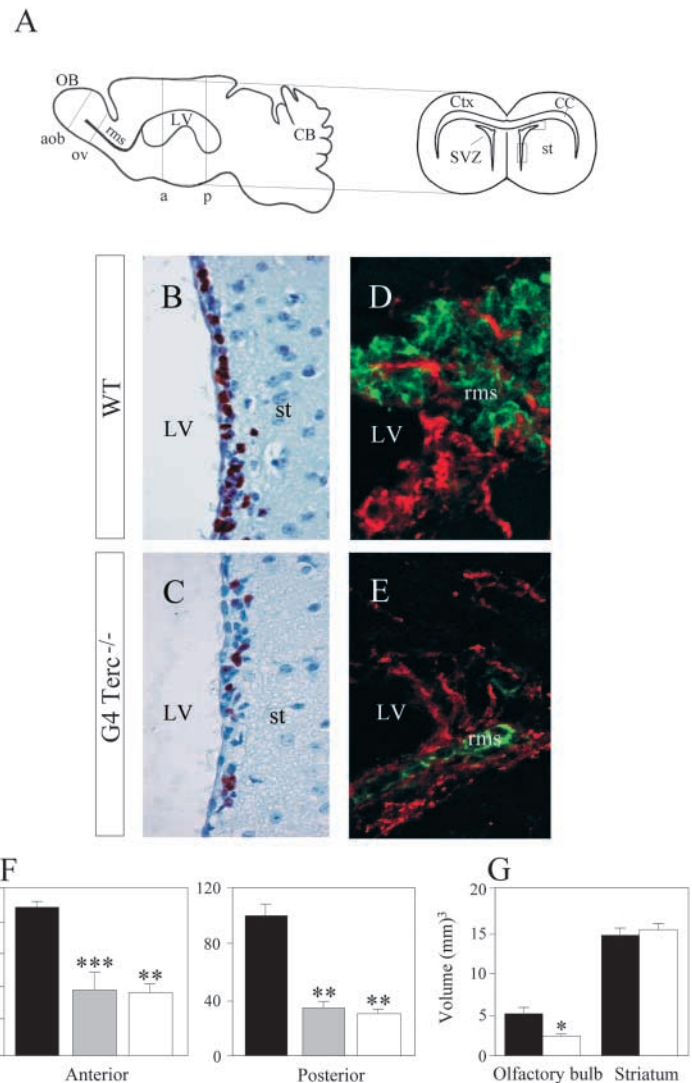
Results

Proliferation of neural progenitors is attenuated in the brain of late generation telomerase-deficient mice

In the adult brain, the SVZ constitutes the most prominent neurogenic germinal niche and forms a thin layer adjacent to the walls of the lateral ventricles right beneath the ependymal layer (reviewed by Alvarez-Buylla and García-Verdugo, 2002; Galli et al., 2003). To determine possible effects of telomere shortening in the proliferation of progenitor populations of the adult brain, we scored all BrdU-positive cells present in the SVZ of wild-type and G2 and G4 *Terc*^{-/-} mice that had been injected seven times with the nucleotide. Because frequency of proliferating cells is not homogeneous along the rostrocaudal extent of the SVZ, being higher in anterior portions (Doetsch et al., 1997), results are presented separately for the most rostral and the most caudal halves of the SVZ (see schematic drawing in Fig. 1A). In animals bred for two or four generations in the absence of an active telomerase there is a dramatic reduction of around 70% in proliferating cells in the SVZ (Fig. 1B,C,F). Reduced numbers of proliferating cells were not accompanied by increased numbers of degenerating cells as we could not detect any difference in labeling with the TUNEL technique in the sections through the SVZ between wild-type and G4 *Terc*^{-/-} mice (data not shown).

Constitutively proliferating progenitor cells labeled with the BrdU administration protocol used here (Morshead et al., 1994) include a population of transit-amplifying progenitor cells (type C cells) as well as their progeny, a population of proliferating neuroblasts (type A cells) (Doetsch et al., 1997; Doetsch et al., 1999) that migrate to the olfactory bulbs (Luskin, 1993; Lois and Alvarez-Buylla, 1994; Galli et al., 2003). Because type A neuroblasts are more frequently found in their migratory route at the dorsolateral corner of the anterior SVZ (see Fig. 1A) (Doetsch et al., 1999), we determined the proportion of BrdU-labeled cells specifically in this region and found a reduction in mutant animals of around 70% relative to control values [mean number of BrdU-labeled cells per section \pm s.e.m.; wild type (WT): 53.6 \pm 16.7, $n=3$ animals; G4 *Terc*^{-/-}: 15.1 \pm 4.7, $n=2$]. Consistent with this dramatic decline in proliferative activity in the SVZ and the rostral migratory stream (rms), labeling of the migrating neuroblasts with anti-PSA-NCAM antibodies appeared reduced (Fig. 1D,E). The reduction in migrating neuroblasts results in a significant decrease in the overall volume of the olfactory bulb in G4 *Terc*^{-/-} animals to more than 50% relative to those of wild type (Fig. 1G). Interestingly, striatal volume was not altered in G4 *Terc*^{-/-} mice, an indication that the reduction in the olfactory bulb was most probably due to a specific reduction in the proliferation of neural progenitor cells in the SVZ postnatally rather than to defects in proliferation or differentiation during embryogenesis (Fig. 1G). Together, these results indicate that proliferation potential of neural progenitors in vivo is decreased in late-generation telomerase-deficient adult mice. Although our data indicate that numbers of migrating neuroblasts (type A cells) were lowered in the *Terc*-deficient mice, we cannot exclude a decrease in the number of type C-cells as well.

Fig. 1. Analysis of the phenotype of the subventricular zone (SVZ) of G2 and G4 *Terc*^{-/-} adult mice in vivo. (A) Schematic diagram of (left) a sagittal section through an adult mouse brain, in which the location and extent of the lateral ventricle (LV) and of the rostral migratory stream (rms) are indicated, and (right) a coronal section through an anterior portion (a) of the lateral ventricle where the SVZ is indicated. OB, olfactory bulb; CB, cerebellum; aob, accessory olfactory bulb; ov, olfactory ventricle; rms, rostral migratory stream; st, striatum; Ctx, cerebral cortex; CC, corpus callosum. The lower boxed area indicates the region shown in B,C. The upper boxed area is the dorsolateral corner of the rms, shown in D and E. (B-E) Coronal sections through the walls of the lateral ventricle (LV) at an anterior level from wild-type (WT) and mutant (G4 *Terc*^{-/-}) mice. (B,C) Detection of BrdU after repetitive pulses over a 12-hour period. Notice the dramatic decrease in the number of cells incorporating the analogue in the mutant, probably the result of reduced proliferation. (D,E) Immunofluorescent images of the rms stained with antibodies to PSA-NCAM (green) and GFAP (red) showing a reduction of labeling in the mutant. (F) Quantification of the total number of BrdU-positive cells per section in the walls of the lateral ventricle in coronal serial sections containing the entire extent of the SVZ. Data are shown as the mean number of immunopositive cells per section \pm s.e.m. of 6 wild-type (black bars), 2 G4 *Terc*^{-/-} mutants (gray bars) and 2 G4 *Terc*^{-/-} mutants (white bars). The length of the SVZ and the size of the BrdU-immunopositive nuclei were the same in all genotypes. Determinations in anterior (a) and posterior levels (p), were done separately because of rostrocaudal differences in proliferating cell frequency. Notice that proliferation is significantly reduced in the mutants at both levels (one-tailed Student's *t*-test: *** $P < 0.001$; ** $P < 0.01$). (G) Bar chart of the volume of the region (see scheme in A) that is rostrocaudally between the accessory olfactory bulb (aob) and of the olfactory ventricle (ov) and the volume of the striatum in wild-type (WT) and mutant (G4 *Terc*^{-/-}) mice. Mutants have a significantly smaller olfactory bulb (one-tailed Student's *t*-test: * $P < 0.05$) but no differences were seen in striatal volume.



Normal development of sensory ganglia and subcortical telencephalon in late generation telomerase-deficient embryos

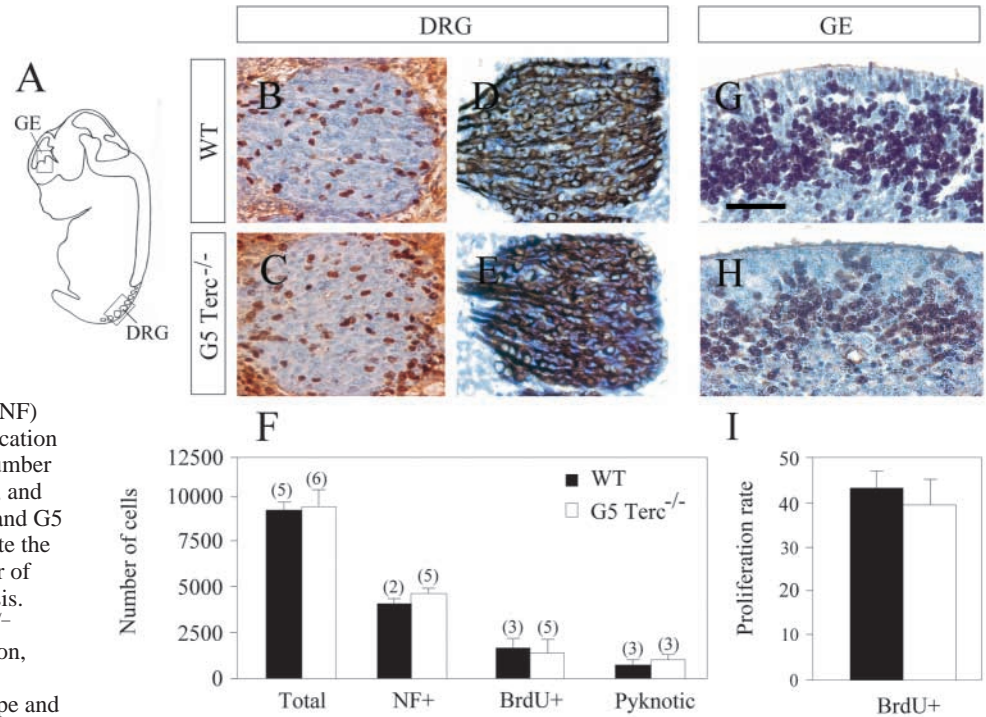
Despite significant reductions in postnatal progenitor populations, the brains of late-generation telomerase-deficient mice are normal in appearance and overall size, suggesting that embryogenesis proceeds normally in these mutants. To determine whether the proliferation, differentiation, and/or survival of embryonic neural precursors is altered by telomere shortening in *Terc* homozygous mutant mice, we analyzed the development of specific neural structures of the PNS and of the CNS in late generation (G5) *Terc*^{-/-} mice. Previous work had indicated that telomerase is expressed in neuroepithelial cells of the developing neural tube of mouse embryos and that telomerase-mediated telomere length maintenance appears to be required for developmentally programmed closure of the neural tube in a certain proportion of late generation *Terc*^{-/-} embryos (Herrera et al., 1999b). Thus, we focused our analysis on the embryonic development of dorsal root ganglia (DRG), since DRG neural and glial progenitors derive from neural crest cells, a population that delaminates from the dorsal neural tube after its closure. In developing DRGs, neurogenesis is initiated

shortly before E10.5 and is complete by E13.5 (Fariñas et al., 1996). We analyzed ganglia from wild-type and G5 *Terc*^{-/-} embryos at E12.5, when neurogenesis peaks and precursor proliferation and differentiation are actively taking place. Complete series of sections through lumbar 1 (L1) DRGs of G5 *Terc*^{-/-} and wild-type embryos were analyzed (Fig. 2). Measurements of BrdU incorporation after a one hour-administration revealed that the numbers and proportions of labeled progenitor cells in G5 *Terc*^{-/-} and wild-type DRGs (Fig. 2B,C,F) were not significantly different. Similarly, there were no differences in the number of differentiated, neurofilament-immunopositive neurons (Fig. 2D-F), in the number or proportion of pyknotic, degenerating cells, or in the total number of cells (Fig. 2F). Together, these results suggest that telomerase deficiency and telomere shortening in G5 *Terc*^{-/-} embryos do not appear to result in defects in the development of neural crest-derived sensory ganglia.

We next analyzed neural progenitor proliferation in the ventricular zone of the ganglionic eminences in G5 *Terc*^{-/-} mice. A histological analysis of Nissl-stained sagittal sections of G5 *Terc*^{-/-} and wild-type E12.5 embryos revealed that the subcortical telencephalon of G5 *Terc*^{-/-} embryos appeared to

Fig. 2. Analysis of dorsal root ganglia (DRG) and ganglionic eminences (GE) in wild-type (WT) and *Terc* mutant E12.5 embryos of the fifth generation (*G5 Terc*^{-/-}).

(A) Schematic diagram of a sagittal section through an E12.5-E14.5 embryo showing the location of lumbar DRGs and ganglionic eminences. (B-F) Analysis of DRG development at the peak of the neurogenic period. (B,C) BrdU immunocytochemical detection in DRGs counterstained with Hematoxylin. (D,E) DRGs immunostained with anti-neurofilament (NF) 150 kDa-specific antibodies. (F) Quantification of the total number of cells, and of the number of neurofilament-positive, BrdU-positive, and apoptotic cells in wild-type (black bars) and *G5 Terc*^{-/-} embryos (white bars). Bars indicate the means \pm s.e.m. obtained from the number of independent embryos shown in parenthesis. DRG development is normal in *G5 Terc*^{-/-} embryos in terms of precursor proliferation, neuronal differentiation and survival. (G-I) Analysis of proliferation in wild-type and mutant ganglionic eminences. Immunodetection of BrdU after a 1 hour pulse in (G) WT and (H) *G5 Terc*^{-/-} embryos, and (I) quantification of the numbers of BrdU-positive cells relative to the total number of cells, as determined in a number of randomly chosen regions of equal size from three wild-type (solid bar) and three *G5 Terc*^{-/-} (white bar) embryos (I). Notice that there are no differences in BrdU labeling index. Scale bar: 100 μ m.



be of normal size and cell density (Fig. 2G,H). We did not observe cell degeneration in sections of *G5 Terc*^{-/-} or wild-type embryonic ganglionic eminences using the TUNEL technique (data not shown). Pregnant females from each genotype received a single injection of BrdU one hour before sacrifice and the proportion of BrdU-positive cells, relative to the total number of cells counted in a fixed area in equivalent sections, was determined (Fig. 2G-I). Proliferation rate in *G5 Terc*^{-/-} embryos appeared normal compared to that in wild type (Fig. 2I), suggesting that the pool of neural progenitors in the ventricular zone and their proliferation rate were not altered in *G5 Terc*^{-/-} embryos with shortened telomeres. Thus, it appears that lack of telomerase activity over several generations does not result in impaired proliferation of neural progenitors of the CNS or the PNS during embryogenesis, in marked contrast to the significant decrease in proliferation of neural progenitor cells in the adult brain.

Embryonic and adult telomerase-deficient NSCs behave differently under the same mitogenic conditions

Because proliferation of adult SVZ progenitors was severely impaired in the *Terc*-deficient animals, we decided to analyze possible effects of the deficiency in the capacity of SVZ cells to generate neurospheres under mitogenic stimulation in vitro (Gritti et al., 1996; Gritti et al., 1999). Although similar numbers of neurospheres were formed from dissociated SVZ tissue of both genotypes (mean number of sphere-forming units/brain \pm s.e.m.: WT, 304 \pm 63; *G4 Terc*^{-/-}, 308 \pm 48, *n*=3 independent cultures), *G4 Terc*^{-/-} primary spheres were 60% smaller after 10 DIV (Fig. 3A). Because each sphere originates

from one cell and because most cells in a neurosphere are not themselves sphere-forming NSCs, the number of spheres formed after a passage can be taken as a reliable estimation of self-renewal capacity. The number of spheres formed relative to the number of cells plated in wild-type and *G4 Terc*^{-/-} secondary cultures were not significantly different (mean percentage \pm s.e.m.: WT, 2.1 \pm 0.4, *n*=3 independent cultures; *G4 Terc*^{-/-}, 1.8 \pm 0.1, *n*=2). However, secondary spheres were also significantly smaller in *G4 Terc*^{-/-} than wild-type spheres (Fig. 3A). To analyze overall growth we determined ratios of cell production after 7 DIV relative to number of cells plated at passages 2 and 3. Growth ratios in the *G4 Terc*^{-/-} cultures were significantly lower than in wild-type cultures (Fig. 3B). This reduction in cell yield is not the consequence of a differential apoptotic response because the frequency of nuclei with apoptotic condensed chromatin was the same in *G4 Terc*^{-/-} (1.3 \pm 0.4%) and wild-type (1.2 \pm 0.7%) neurospheres. Because these data suggest that limited growth of mutant NSCs is caused by slower proliferation, we sought to determine proliferation rates. BrdU incorporation was significantly reduced in *G4 Terc*^{-/-} neurospheres compared with wild-type ones (Fig. 3C,D; see Fig. 5C for quantification). Thus, NSCs isolated from the adult SVZ appear to proliferate more slowly than wild-type NSCs.

In contrast, NSCs isolated from E14.5 wild-type and *G5 Terc*^{-/-} embryos, and grown in vitro under the same mitogenic stimulation, did not appear to differ in their proliferative potential. Both genotypes yielded equivalent numbers of neurospheres that appeared to grow equally well, resulting in indistinguishable growth curves (Fig. 4A-D). Self-renewal appeared to be equivalent in *G5 Terc*^{-/-} and wild-type embryos,

Fig. 3. In vitro growth kinetics of wild-type (WT) and G4 *Terc*^{-/-} adult NSCs (*n*=3 independent cultures). (A) G4 *Terc*^{-/-} primary and secondary spheres were much smaller than wild-type spheres as shown by a shift to the left in the size distribution (left). Phase contrast micrographs and mean average diameter (in $\mu\text{m} \pm \text{s.e.m.}$) of floating neurospheres (right). Diameter is significantly lower (one-tailed Student's *t*-test, $P < 0.001$) in G4 *Terc*^{-/-} NSCs when compared to wild-type NSCs. (B) Fold increase in the number of cells 7 DIV after passage 2 (P2) and 3 (P3) is dramatically reduced in G4 *Terc*^{-/-} (white bars) relative to wild-type (black bars) cells (one-tailed Student's *t*-test, $P < 0.05$). (C) There are less BrdU-positive cells (red) relative to the total number of cells (DAPI stain) in mutant spheres (see quantifications in Fig. 5). Scale bars: A, 200 μm ; C,D, 50 μm .

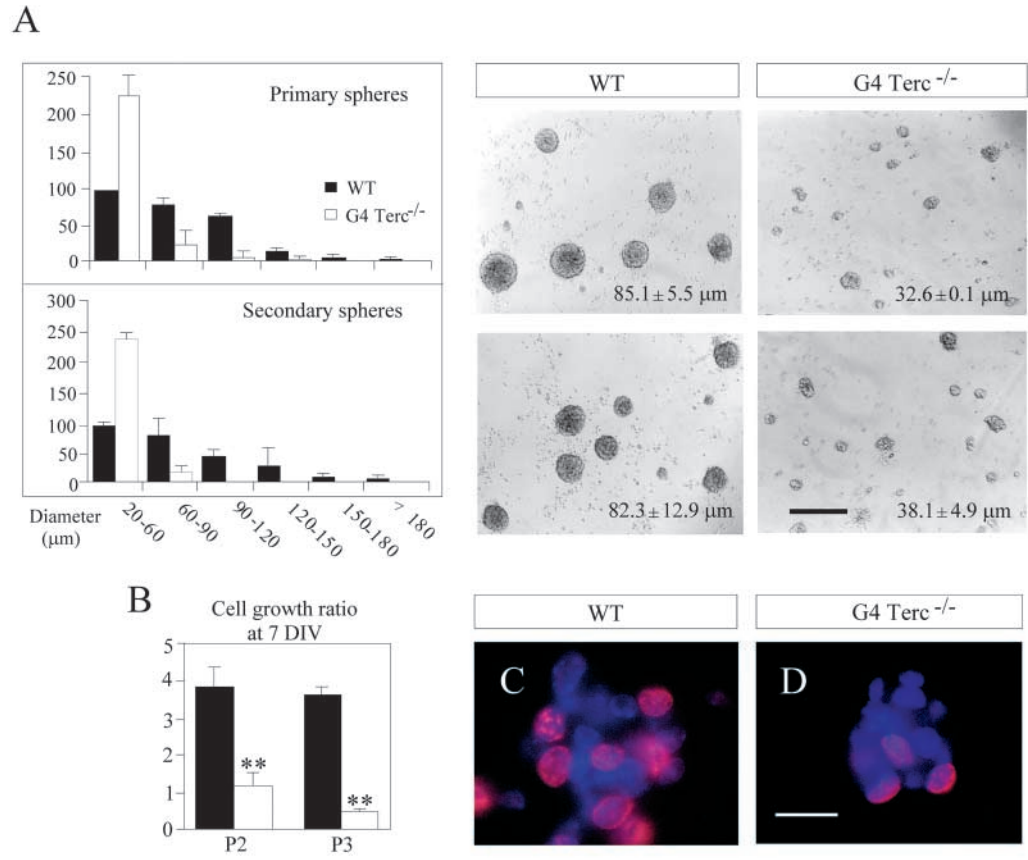
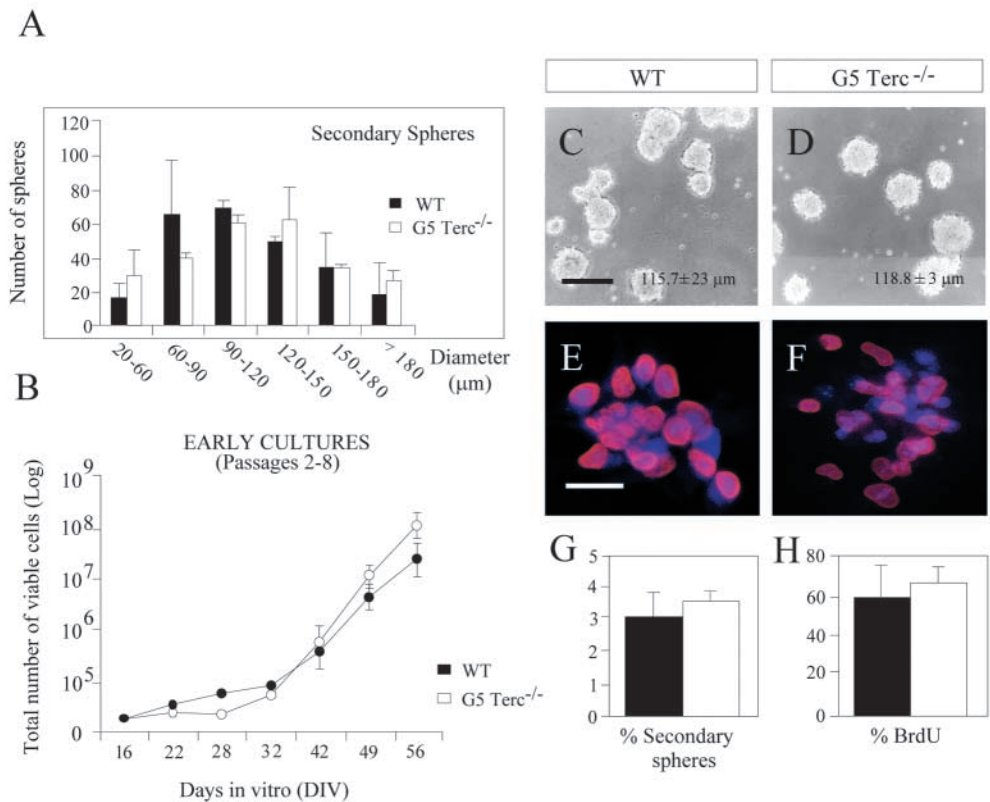


Fig. 4. In vitro growth kinetics of wild-type (WT) and G5 *Terc*^{-/-} embryonic NSCs (*n*=3 independent cultures). (A) Size distribution of secondary spheres formed after 6 DIV showing no differences between wild-type and G5 *Terc*^{-/-} cultures. (B) Cell growth in passages 2-8 (early cultures) is the same in both genotypes. (C,D) Phase contrast micrographs and mean average diameter of secondary neurospheres from wild-type and G5 *Terc*^{-/-} embryonic cultures. (E,F) Representative photomicrographs showing immunofluorescent detection of BrdU incorporation (red) and DAPI staining (blue) in wild-type (WT) and G5 *Terc*^{-/-} secondary neurospheres. (G) Percentages of secondary spheres formed out of an equivalent number (10,000 cells) of dissociated wild-type (black bars) and G5 *Terc*^{-/-} (white bars) in early cultures, showing no apparent differences between the two genotypes. (H) Proliferation rates for wild-type (black bars) and G5 *Terc*^{-/-} (white bars). Mutant NSCs have a normal proliferation rate. Scale bars: C,D, 200 μm ; E,F, 50 μm .



as equal number of sphere-forming units were found in both genotypes (Fig. 4G). There was no difference between the genotypes in the average size or distribution of secondary spheres grown for 6 DIV (Fig. 4A). There were also no differences in the proportions of apoptotic cells as seen by DAPI chromatin staining (mean percentage \pm s.e.m.: WT, 1.1 ± 1.1 ; G5 *Terc*^{-/-}, 0.8 ± 1.1) or cells that incorporated BrdU (Fig. 4E,F,H). Together, these results indicate that proliferation, survival and self-renewal of embryonic NSC cultures are not compromised in G5 *Terc*^{-/-} mice.

Differences in the proliferative behavior between G5 embryonic and G4 adult *Terc*^{-/-} NSCs could relate to a differential severity in telomere erosion. For each new generation in the telomerase-deficient strain, the starting values of telomere lengths are those found in the zygote (Blasco et

al., 1997). However, because the number of cell divisions in different somatic lineages may vary dramatically, telomere sizes need to be determined for each cell type under analysis. Therefore, we measured telomere length in adult and embryonic NSCs by Q-FISH with a Cy-3 labeled telomere-specific probe. Because of the small number of cells available and the low number of mitosis in the G4 adult mutant cultures, telomere lengths were measured at interphase. In wild-type cultures, average telomere lengths were higher in embryonic NSCs than in adult NSCs (Fig. 5A), an indication that adult cells may go through many more rounds of cell division during the life of the animal. When telomerase-deficient cells were compared with wild type cells, an overall similar reduction of 60-70% in average telomere length was found in both G5 embryonic and G4 adult mutant NSCs (Fig. 5A). Thus,

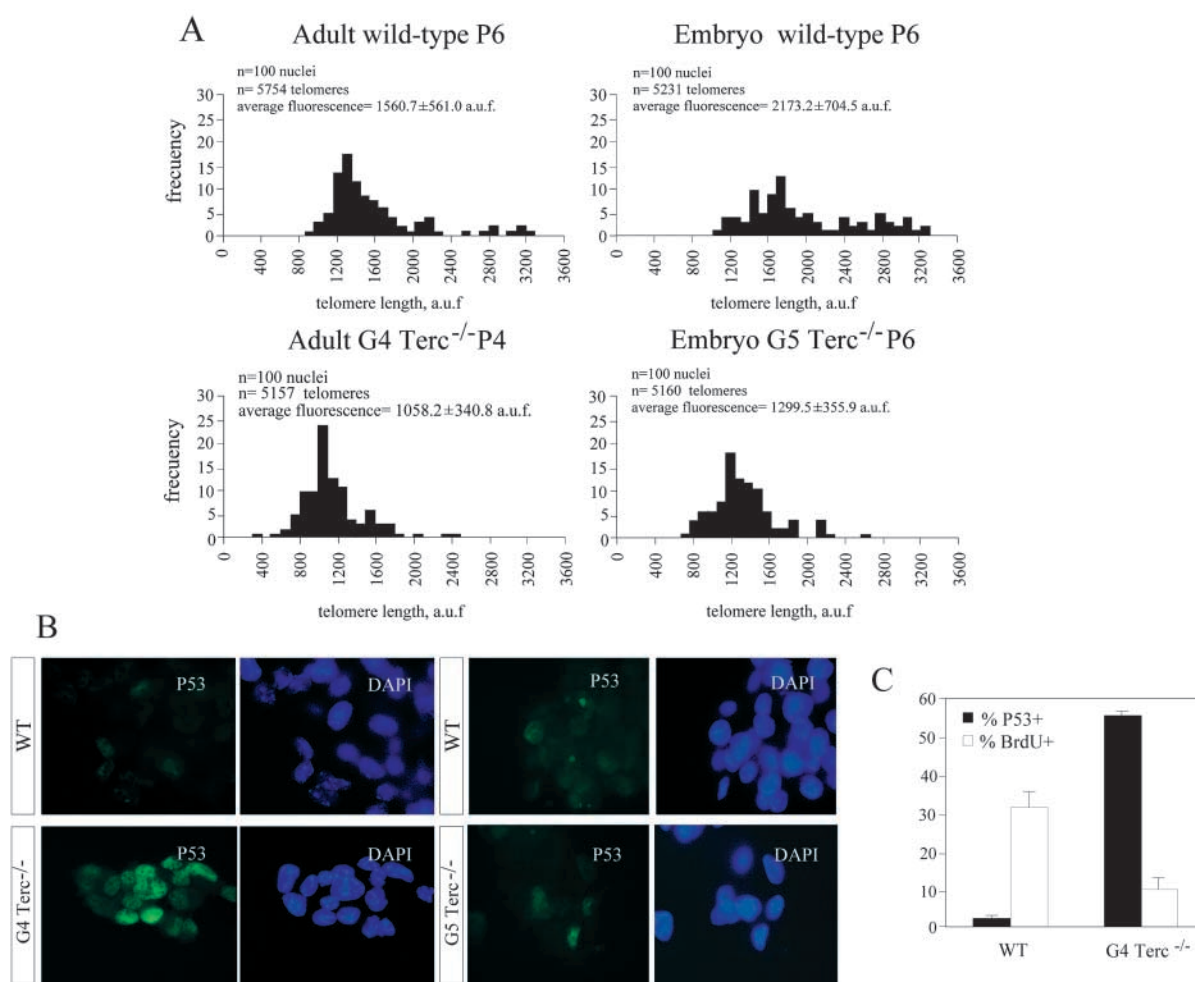


Fig. 5. (A) Telomere length distribution by Q-FISH analysis in interphase nuclei of wild-type and *Terc*^{-/-} G4 adult- and G5 embryo-derived cells in early cultures. Measurements are given in arbitrary units of fluorescence (a.u.f.). A shift to the left in the size distribution of telomerase-deficient compared to wild-type cells indicates a significantly higher proportion of telomeres with lower fluorescence signals. An average reduction in telomere length of around 60% is observed in both adult and embryonic telomerase-deficient cells. (B) Photomicrographs showing immunofluorescent detection of p33 (green) and DAPI staining (blue) in adult wild-type (WT) and G4 *Terc*^{-/-} neurospheres (left) and in embryonic wild-type (WT) and G5 *Terc*^{-/-} neurospheres (right). Wild-type neurospheres did not express detectable levels of p33 after 15 DIV. However, primary neurospheres derived from G4 *Terc*^{-/-} adult mice cultured for the same time showed nuclear p33 staining. No signs of apoptosis were observed. p33 immunostaining of embryonic wild-type and G5 *Terc*^{-/-} neurospheres after 15 DIV showed no detectable p33 protein. (C) Percentages of p33 and BrdU immunopositive cells in the adult neurospheres of both genotypes showing an inverse relationship. Immunodetections were performed separately because p33 could not be detected by the primary antibody after the acid treatment needed for BrdU immunocytochemistry. Parallel staining in spheres obtained from p33 null mice yielded no fluorescence at all (data not shown).

embryonic and adult NSCs from telomerase-deficient mice of late generation have significantly reduced telomere lengths. However, telomere lengths in embryonic mutant NSCs were longer than in adult mutant NSCs. Therefore, the differential proliferative response of mutant embryonic and adult NSCs might be attributed to a higher degree of telomere erosion in adult NSCs.

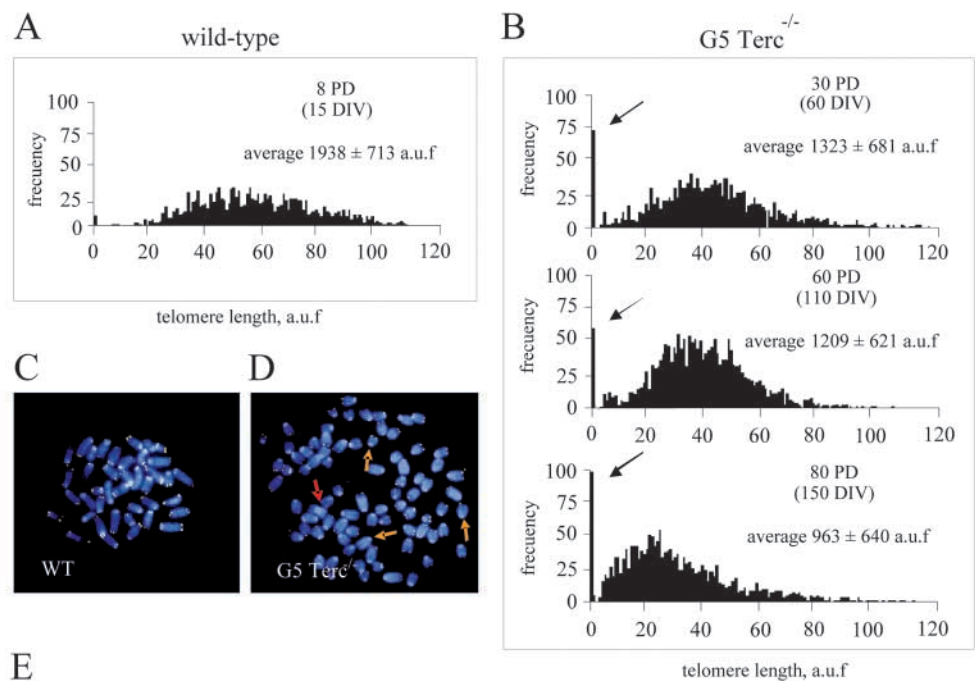
Because shortened dysfunctional telomeres appear to trigger signaling pathways associated with damaged DNA (Espejel et al., 2002a; Espejel et al., 2002b; Goytisolo and Blasco, 2002; Smogorzewska et al., 2002; d'Adda di Fagagna et al., 2003; Takai et al., 2003), we examined whether telomere length reductions found in adult NSCs resulted in the activation of DNA damage responses that were not active in embryonic NSCs with longer telomeres. Telomere shortening and associated chromosomal instability in late generation *Terc*^{-/-} adult mice had been previously shown to correlate with increased proportions of cells expressing p53 and, therefore, p53 upregulation is considered to be an indication of the presence of dysfunctional telomeres (Chin et al., 1999; Leri et al., 2003). Moreover, activation of p53 appears to mediate the adverse effects of critically short telomeres on the proliferation

and survival in different cell types (Chin et al., 1999; González-Suárez et al., 2002; Leri et al., 2003). To evaluate if telomeric erosion found in embryonic and adult NSCs was equivalent in terms of p53 activation we immunostained neurospheres for p53 (Fig. 5B). Neurospheres derived from G4 *Terc*^{-/-} adult mice showed an increase in the number of p53 immunopositive nuclei (Fig. 5B). However, p53 protein was undetectable in embryonic wild-type and G5 *Terc*^{-/-} neurospheres under the same conditions (Fig. 5B). Therefore, it appears that p53 is upregulated in early cultures of mutant G4 adult NSCs but not of G5 embryonic NSCs, suggesting that telomere reductions in embryonic G5 mutant NSCs may not be sufficient to activate a DNA damage response.

Because activation of p53 induces either cell cycle arrest or apoptotic cell death (for a review, see Vogelstein et al., 2000), it is likely that the hypocellularity observed in G4 *Terc*^{-/-} cultures is the result of a nuclear increase in p53 levels. In agreement with this proposal, an inverse correlation was observed between the percentage of p53-immunopositive cells and the percentage of cells in S-phase (Fig. 5C). DAPI-stained chromatin condensations indicative of apoptosis were rare in both wild-type and mutant cultures, an indication that in adult

Fig. 6. Telomere length distribution by Q-FISH analysis in wild-type (A) and G5 *Terc*^{-/-} (B) embryo-derived metaphases at different times in culture (DIV, days in vitro; PD, population doublings). Measurements are given in a.u.f. A shift to the left in the size distribution of telomerase-deficient cells with replication in vitro indicates a significantly higher proportion of telomeres with lower fluorescence signals. Notice the increase in the frequency of undetectable telomeres that show no fluorescent signal (sensitivity of the assay, around 200 bp; see E for quantification).

(C,D) Representative photomicrographs of wild-type and aneuploid G5 *Terc*^{-/-} DAPI-stained metaphases (blue) after hybridization with a Cy3-labeled telomeric probe (yellow). Notice decreased signal intensity as well as undetectable telomeres (red arrows) in G5 *Terc*^{-/-} chromosomes. (E) Cytogenetic analysis in embryonic wild-type and G5 *Terc*^{-/-} NSCs during expansion in vitro. Table shows the number of cytogenetic abnormalities per metaphase. Notice their increase with time in culture in the absence of telomerase (see example of a Robertsonian fusion in D, yellow arrows).



	undetectable telomeres (%)	Cytogenetic abnormalities			
		Robertsonian	end-to-end fusions dicentric	p-to-q arm	complex abnormalities (rings, fragments, ...)
wild-type 8 PD (15 DIV)	0.63	0	0	0	0
G5 <i>Terc</i> ^{-/-} 30 PD (60 DIV)	4.83	1.18	0.02	0.02	0
60 PD (110 DIV)	2.96	0.40	0.08	0	0.24
80 PD (150 DIV)	5.32	1.52	0	0.04	0.24

NSCs telomere dysfunction results in cell cycle arrest but not cell death.

Embryonic NSCs with very short telomeres, cytogenetic abnormalities, and nuclear p53 accumulation proliferate extensively in vitro

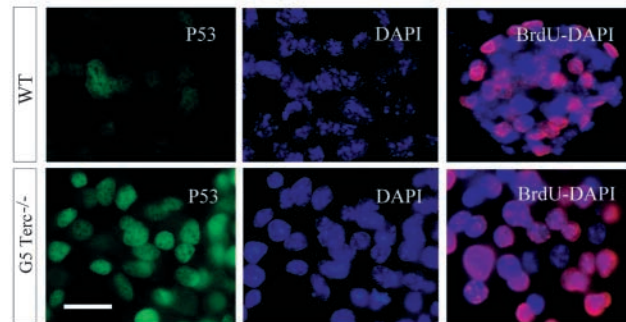
In order to determine whether normal cellularity and absence of nuclear p53 accumulation was indeed related to the presence of sufficiently long telomeres in NSCs isolated from mutant embryos, we analyzed embryonic cultures after extensive proliferation in vitro. Studies in stem cells of other tissue types, such as hematopoietic, indicate that telomerase deficiency may not impair proliferation under steady-state conditions but that it is detrimental for high demand proliferative challenges (Samper et al., 2002). Mutant NSCs were collected at different time points in long-term cultures and telomere lengths were measured using Q-FISH during metaphase (Fig. 6A,B). Using metaphasic Q-FISH for telomeric sequences it is possible to determine telomere length distribution as well as the frequency of chromosomes with very short, undetectable telomeres (length <200 bp; see proportions in histograms and in Fig. 6E) and chromosomal abnormalities (Fig. 6C-E). With time in culture, the telomeres of telomerase-incompetent cells shortened and the percentage of undetectable telomeres and of cytogenetic abnormalities increased significantly (Fig. 6).

To determine whether p53 was induced in embryonic NSCs in response to telomere dysfunction and chromosomal instability we immunostained embryonic G5 mutant NSCs after 110 DIV, when they showed an increased percentage of undetectable telomeres and chromosomal aberrations (Fig. 6C-E). Virtually all G5 mutant NSCs were strongly immunoreactive for nuclear p53 (Fig. 7A). Surprisingly, cells in these spheres incorporated BrdU in a similar way to wild-type cells, an indication that, despite increased expression of the tumor suppressor protein, these cells proliferate normally (Fig. 7C). Consistent with a normal BrdU labeling index in mutant spheres, long-term cultures of wild-type and G5 *Terc*^{-/-} NSCs had indistinguishable growth curves (Fig. 7B). Thus, embryonic NSCs proliferate extensively in culture and maintain their self-renewal and replicative capacity despite the presence of telomere-exhausted chromosomes, which are likely to be dysfunctional as indicated by the increased numbers of end-to-end chromosomal fusions and nuclear p53 accumulation. Altogether, these results suggest a fundamental difference between adult and embryonic NSCs in terms of their proliferative response to the activation of p53 induced by the presence of short and dysfunctional telomeres.

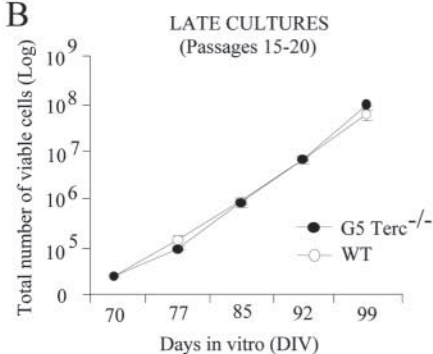
Discussion

We have explored the effects of telomere attrition in the behavior of murine neural progenitors. Our results from a mouse strain engineered to lack the RNA component of telomerase indicate that, in the absence of telomerase activity for several generations telomere erosion, concomitant with an increase in the level of the p53 protein, can abrogate proliferation of adult NSCs, and that embryonic NSCs are

A



B



C

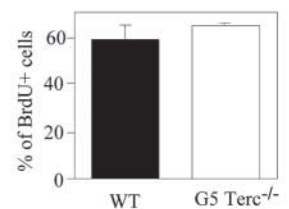


Fig. 7. (A) Photomicrographs showing immunofluorescent detection of BrdU incorporation (red), p53 (green) and DAPI staining (blue) in embryonic wild-type (WT) and G5 *Terc*^{-/-} NSCs cultured for 110 DIV. Most nuclei in mutant neurospheres were immunoreactive for p53 while only a few wild type were positive. In spite of high levels of p53 protein, most G5 *Terc*^{-/-} cells cultured for 110 DIV incorporated BrdU (see quantification in C). No signs of apoptosis are observed. (B) Cell growth in passages 15 to 20 (late cultures) is the same in both genotypes. Scale bar: 100 μ m.

capable of extensive proliferation in the presence of shortened telomeres and increased levels of nuclear p53.

Cell-intrinsic limitation of proliferative life-span to a finite number of divisions is a characteristic of most somatic human cells and it is dependent on progressive shortening of telomeres to the point of loss of chromosomal end integrity (see Blackburn, 2000). Therefore, telomere maintenance is essential, particularly in highly proliferative cell populations. In contrast to human primary cells, cells from inbred mouse strains do not appear to undergo telomere-mediated replicative senescence under normal conditions because they have very long telomeres (40-60 kbp) compared to humans and to wild mice (5-10 kbp) (Prowse and Greider, 1995; Blasco et al., 1997). Nevertheless, the effects of telomere shortening in different types of cells can be analyzed in the *Terc*-deficient strain, in which critical reductions in telomere lengths have been shown to result in deleterious cellular phenotypes after extensive culture or after several generations of mice (Blasco et al., 1997; Rudolph et al., 1999; Niida et al., 2000; Espejel and Blasco, 2002a; Espejel and Blasco, 2002b). After four to six generations without telomerase activity in laboratory mice, telomeres approach the size of those found in human cells and effects of telomere attrition can be investigated. Proliferative

defects have been observed in germinal centers, skin and the hematopoietic system and fibroblasts of late generation telomerase-deficient mice, which are consistent with telomere-dependent premature senescent-like growth arrest or apoptosis (Lee et al., 1998; Rudolph et al., 1999; Samper et al., 2002; Espejel and Blasco, 2002a; Espejel and Blasco, 2002b). As shown in the present study adult neural progenitors are also sensitive to telomere shortening (Wong et al., 2003) but, surprisingly, embryonic neural progenitors with critically short telomeres proliferate normally.

The reduced capacity for proliferation of adult NSCs is found in the *in vivo* natural steady-state condition, in the absence of any exogenous mitogenic stimulation. Moreover, large significant reductions in the number of proliferating cells in the SVZ is observed in the mutants as early as in the second breeding generation, when most chromosomes are still sufficiently long. A formal possibility to explain this result is that telomerase activity itself contributes to cell cycle dynamics in adult NSCs. A possible role of telomerase activity in the regulation of proliferation in cells with sufficiently long telomeres has been suggested by the fact that G1 *Terc*^{-/-} are less prone to skin tumor formation and that telomerase overexpression in epithelial cells makes them more susceptible to mitogenic stimulation and tumor formation (González-Suárez et al., 2000; González-Suárez et al., 2001; González-Suárez et al., 2002; Artandi et al., 2002; Smith et al., 2003). In the nervous system, pharmacological inhibition of telomerase activity decreases FGF2-induced proliferation of cortical precursor cells (Haik et al., 2000), suggesting that telomerase activity may be linked to cell cycling regulation in certain neural progenitors, although possible mechanisms for these actions are presently unclear (for a review, see Blasco, 2002). The other possibility is that adult NSCs might be extremely sensitive to erosion of particular chromosomes (see Hemann et al., 2001). The involvement of telomere shortening in the growth retardation of G4 mutant NSCs *in vitro* are supported by the observation that proliferation deficits correlate with a rise in the detectable levels of nuclear p53. Further support for a direct effect of telomere erosion, even at G2, in the proliferation of these cells is provided by recent data showing that BrdU incorporation in the SVZ of G1 *Terc*-deficient mice, which lack telomerase activity but have longer telomeres, is not decreased (Wong et al., 2003).

Despite the fact that proliferation rates were substantially reduced in telomerase-deficient brains we could recover the same number of neurosphere-forming cells from the SVZ of adult telomerase-deficient mice as from wild-type SVZ, an indication that stem cell state is not affected by the lack of telomerase activity or by telomere shortening. Moreover, stem cell renewal appears to be also preserved in culture, as the proportions of sphere forming units at each passage are similar in wild-type and mutant cultures despite reduced numbers of cells produced per neurosphere upon growth factor stimulation. Thus, our results suggest that proliferation and maintenance of the stem cell state are regulated intrinsically by distinct signals (Tropepe et al., 1997; Shimazaki et al., 2001).

When telomeres become sufficiently short to compromise their interaction with specific telomere-binding proteins, they are recognized as damaged DNA (see d'Adda di Fagagna et al., 2003; Takai et al., 2003). This results in the activation of the non-homologous end-joining pathway for double strand break repair,

which mediates some of the outcomes of telomere dysfunction (Espejel et al., 2002a; Espejel et al., 2002b; Goytisolo and Blasco, 2002; Smogorzewska et al., 2002) and the ARF/p53 and the p16/Rb signaling pathways for growth arrest or apoptosis (Harley et al., 1990; Vaziri et al., 1994; Chin et al., 1999). p53 immunoreactivity is generally low, as this tumor-suppressor protein is relatively short-lived, but several types of DNA damage, including telomere erosion, can activate p53 and result in a rapid increase in the level of nuclear p53 and the transcriptional activation of genes that induce cell cycle arrest or apoptosis depending on the cell types (Vogelstein et al., 2000). In our NSC cultures, p53 up-regulation is observed in adult NSCs with shortened telomeres, in agreement with the importance of the p53 pathways for the murine response to telomere damage (Chin et al., 1999). In murine cells telomere damage signaling appears to be transduced only through the p53 pathway because, in contrast to p53-deficient human cells, mouse cells that lack p53 do not arrest, suggesting that other pathways such as activation of p16 may be dispensable (Smogorzewska and de Lange, 2002). Consistently, p53 deficiency can rescue many of the phenotypes of late generation *Terc*^{-/-} mice and extend strain viability and fertility into the eight generation (Chin et al., 1999). The observation that culture itself is not inducing p53 in wild-type cells suggests that its activation is specifically induced by DNA damage at telomeres. The p53 upregulation is coincidental with growth impairment in the adult NSCs, suggesting induction of a p53 checkpoint arrest.

The proliferation rate of mutant embryonic cells, however, remained constant with continual passaging, despite the fact that aneuploidy and chromosome rearrangements were frequently detected in these NSC cultures, and p53 levels increased in virtually all nuclei. Cells can escape replicative senescence by acquiring inactivating mutations in cell cycle checkpoint regulating genes, most characteristically p53, that lead to continued proliferation and, most frequently, to a final crisis associated with extreme telomere erosion and massive chromosomal instability (Sherr and DePinho, 2000). Only rare survivors could emerge from crisis and proliferate indefinitely, possibly by activation of alternative telomere elongation mechanisms such as ALT (see Kass-Eissler and Greider, 2000). Nevertheless, we have not detected any crisis events in our cultures and, moreover, all three independent cultures behaved similarly suggesting that mutation of p53 is unlikely to explain the normal growth of all G5 *Terc*^{-/-} mutant cultures.

The mechanisms that regulate p53 transcriptional activity are now beginning to be understood and include both post-translational modifications and alterations in p53 binding proteins (Giaccia and Kastan, 1998; Brooks and Gu, 2003). Interactions with coactivators such as p300/CBP, PCAF, Sp1 or Ets1 that are required to form stable DNA-p53 transcription initiation complexes appear to be modulated by phosphorylation. Moreover, activation of the complexes appears to be subject to regulation by acetylation (Giaccia and Kastan, 1998; Barlev et al., 2001; Xu et al., 2002; Brooks and Gu, 2003). Therefore, cell context differences in the expression of coactivators or in the signaling pathways upstream of p53 modifications could underlie ontogeny-related changes in the response of NSCs to alterations in telomerase activity and telomere lengths. Interestingly, silencing of p53 transcriptional activity by NAD⁺-dependent histone deacetylases of the Sir2 family suggests that cell metabolism may influence final cell

fate decisions during cellular stresses, including DNA damage, and underscores the importance of cell context and activity (Langley et al., 2002; Vaziri et al., 2001; Luo et al., 2001; Brooks and Gu, 2003). Embryonic neural precursor cells have been shown to be relatively resistant to deficits in DNA repair molecules that play a role in nervous system development. Mouse strains deficient in members of the non-homologous end-joining mechanism for double strand break repair, such as Ku70, Ku80, XRCC4 or Lig4, are characterized by defective neurogenesis during embryogenesis as a result of increased apoptosis in postmitotic neuronal populations, but not in their progenitor populations (see Gao et al., 1998; Gu et al., 2000).

In conclusion, we have shown that proliferative potential of NSCs residing in the adult brain is subject to tight intrinsic regulation and, therefore, more knowledge will be needed on intracellular mechanisms of cycling control if we are to pursue the reactivation of latent NSC populations to engage endogenous neurogenesis for the treatment of brain disease. Moreover, embryonic NSCs can escape cellular check points and, therefore, methods to monitor genetic stability of ex vivo expanded neural stem cells will be necessary prior to any therapeutic intervention.

We thank A. Vescovi and A. Gritti for their invaluable advice and help with the culture of neural stem cells. We also thank R. Serrano, E. Santos and E. Samper in M.A.B.'s laboratory for mouse care, genotyping and BrdU injections, respectively, J. Pertusa for help with cell counting and stereology and comments to the manuscript. This work was supported by grants from Ministerio de Ciencia y Tecnología (MCYT) (SAF99-0119-C02-01, SAF-2002-03355 and IFD97-2153), Fundació La Marató de TV3 and Ministerio de Sanidad y Consumo (G03/210), Spain, to I.F. Research in M.A.B.'s laboratory is funded by grants SAF2001-1869 and GEN2001-4856-C13-08 from the MCYT, grant 08.1/0030/98 from the regional government of Madrid, by grants FIGH CT 1999-00009, FIGH-CT-1999-00002, QLGI 1999-01341 and FIGH-CT-2002-00217 from the European Union, by the Swiss Bridge Cancer Award 2000 and by the DIO. The DIO was founded and is supported by the Spanish Research Council (CSIC) and by Pharmacia. S.F. is a predoctoral fellow of the Fondo de Investigaciones Sanitarias. M.C.-J. is a predoctoral fellow of the Generalitat Valenciana and E.B. is a fellow of the predoctoral FPI Program (MCYT).

References

- Alvarez-Buylla, A. and Garcia-Verdugo, J. M. (2002). Neurogenesis in adult subventricular zone. *J. Neurosci.* **22**, 629-634.
- Artandi, S. E., Alson, S., Tietze, M. K., Sharpless, N. E., Ye, S., Greenberg, R. A., Castrillon, D. H., Horner, J. W., Weiler, S. R., Carrasco, R. D. and DePinho, R. A. (2002). Constitutive telomerase expression promotes mammary carcinomas in aging mice. *Proc. Natl. Acad. Sci. USA* **99**, 8191-8196.
- Barlev, N. A., Liu, L., Chehab, N. H., Mansfield, K., Harris, K. G., Halazonetis, T. D. and Berger, S. L. (2001). Acetylation of p53 activates transcription through recruitment of coactivators/histone acetyltransferases. *Mol. Cell* **8**, 1243-1254.
- Blackburn, E. H. (2000). Telomere states and cell fates. *Nature* **408**, 53-56.
- Blasco, M. A., Lee, H. W., Hande, M. P., Samper, E., Lansdorp, P. M., DePinho, R. A. and Greider, C. W. (1997). Telomere shortening and tumor formation by mouse cells lacking telomerase RNA. *Cell* **91**, 25-34.
- Blasco, M. A. (2002). Telomerase beyond telomeres. *Nat. Rev. Cancer* **2**, 627-633.
- Bodnar, A. G., Ouellette, M., Frolkis, M., Holt, S. E., Chiu, C. P., Morin, G. B., Harley, C. B., Shay, J. W., Lichtsteiner, S. and Wright, W. E. (1998). Extension of life-span by introduction of telomerase into normal human cells. *Science* **279**, 349-352.
- Brooks, C. L. and Gu, W. (2003). Ubiquitination, phosphorylation and acetylation: the molecular basis for p53 regulation. *Curr Opin Cell Biol.* **15**, 164-171.
- Caporaso, G. L., Lim, D. A., Alvarez-Buylla, A. and Chao, M. V. (2003). Telomerase activity in the subventricular zone of adult mice. *Mol. Cell Neurosci.* **23**, 693-702.
- Chin, L., Artandi, S. E., Shen, Q., Tam, A., Lee, S. L., Gottlieb, G. J., Greider, C. W. and DePinho, R. A. (1999). p53 deficiency rescues the adverse effects of telomere loss and cooperates with telomere dysfunction to accelerate carcinogenesis. *Cell* **97**, 527-538.
- Chiu, C. P. and Harley, C. B. (1997). Replicative senescence and cell immortality: the role of telomeres and telomerase. *Proc. Soc. Exp. Biol. Med.* **214**, 99-106.
- d'Adda di Fagnana, F., Reaper, P. M., Clay-Farrace, L., Fiegler, H., Carr, P., Von Zglinicki, T., Saretzki, G., Carter, N. P. and Jackson, S. P. (2003). A DNA damage checkpoint response in telomere-initiated senescence. *Nature* **426**, 194-198.
- de Lange, T. (2002). Protection of mammalian telomeres. *Oncogene* **21**, 532-540.
- Doetsch, F., Garcia-Verdugo, J. M. and Alvarez-Buylla, A. (1997). Cellular composition and three-dimensional organization of the subventricular germinal zone in the adult mammalian brain. *J. Neurosci.* **17**, 5046-5061.
- Doetsch, F., Caille, I., Lim, D. A., Garcia-Verdugo, J. M. and Alvarez-Buylla, A. (1999). Subventricular zone astrocytes are neural stem cells in the adult mammalian brain. *Cell* **97**, 703-716.
- Espejel, S., Franco, S., Segura, A., Gae, D., Bailey, S. M., Taccioli, G. E. and Blasco, M. A. (2002b). Functional interaction between DNA-PKcs and telomerase in telomere length maintenance. *EMBO J.* **21**, 6275-6287.
- Fariñas, I., Yoshida, C. K., Backus, C. and Reichardt, L. F. (1996). Lack of neurotrophin-3 results in death of spinal sensory neurons and premature differentiation of their precursors. *Neuron* **17**, 1065-1078.
- Fu, W., Killen, M., Culmsee, C., Dhar, S., Pandita, T. K. and Mattson, M. P. (2000). The catalytic subunit of telomerase is expressed in developing brain neurons and serves a cell survival-promoting function. *J. Mol. Neurosci.* **14**, 3-15.
- Gage, F. H. (2000). Mammalian neural stem cells. *Science* **287**, 1433-1438.
- Galli, R., Gritti, A., Bonfanti, L. and Vescovi, A. L. (2003). Neural stem cells: an overview. *Circ Res.* **92**, 598-608.
- Gao, Y., Sun, Y., Frank, K. M., Dikkes, P., Fujiwara, Y., Seidl, K. J., Sekiguchi, J. M., Rathbun, G. A., Swat, W., Wang, J. et al. (1998). A critical role for DNA end-joining proteins in both lymphogenesis and neurogenesis. *Cell* **95**, 891-902.
- Giacca, A. J. and Kastann M. B. (1998). The complexity of p53 modulation: emerging patterns from divergent signals. *Genes Dev.* **12**, 2973-2983.
- González-Suárez, E., Samper, E., Ramírez, A., Flores, J. M., Martín-Caballero, J., Jorcano, J. L. and Blasco, M. A. (2001). Increased epidermal tumors and increased skin wound healing in transgenic mice overexpressing the catalytic subunit of telomerase, mTERT, in basal keratinocytes. *EMBO J.* **20**, 619-630.
- González-Suárez, E., Flores, J. M. and Blasco, M. A. (2002). Cooperation between p53 mutation and high telomerase transgenic expression in spontaneous cancer development. *Mol. Cell. Biol.* **22**, 7291-7301.
- Goytisolo, F. A. and Blasco, M. A. (2002). Many ways to telomere dysfunction: in vivo studies using mouse models. *Oncogene* **21**, 584-591.
- Greenberg, R. A., Allsopp, R. C., Chin, L., Morin, G. B. and DePinho, R. A. (1998). Expression of mouse telomerase reverse transcriptase during development, differentiation and proliferation. *Oncogene* **16**, 1723-1730.
- Greider, C. W. (1998). Telomeres and senescence: the history, the experiment, the future. *Curr. Biol.* **8**, 178-181.
- Gritti, A., Parati, E. A., Cova, L., Frolichsthal, P., Galli, R., Wanke, E., Faravelli, L., Morassutti, D. J., Roisen, F., Nickel, D. D. and Vescovi, A. L. (1996). Multipotential stem cells from the adult mouse brain proliferate and self-renew in response to basic fibroblast growth factor. *J. Neurosci.* **16**, 1091-1100.
- Gritti, A., Frolichsthal-Schoeller, P., Galli, R., Parati, E. A., Cova, L., Pagano, S. F., Bjornson, C. R. and Vescovi, A. L. (1999). Epidermal and fibroblast growth factors behave as mitogenic regulators for a single multipotent stem cell-like population from the subventricular region of the adult mouse forebrain. *J. Neurosci.* **19**, 3287-3297.
- Groszer, M., Erickson, R., Scripture-Adams, D. D., Lesche, R., Trumpp, A., Zack, J. A., Kornblum, H. I., Liu, X. and Wu, H. (2001). Negative regulation of neural stem/progenitor cell proliferation by the Pten tumor suppressor gene in vivo. *Science* **294**, 2186-2189.
- Gu, Y., Sekiguchi, J., Gao, Y., Dikkes, P., Frank, K., Ferguson, D., Hasty,

- P., Chun, J. and Alt, F. W. (2000). Defective embryonic neurogenesis in Ku-deficient but not DNA-dependent protein kinase catalytic subunit-deficient mice. *Proc. Natl. Acad. Sci. USA* **97**, 2668-2673.
- Haik, S., Gauthier, L. R., Granotier, C., Peyrin, J. M., Lages, C. S., Dormont, D. and Boussin, F. D. (2000). Fibroblast growth factor 2 up regulates telomerase activity in neural precursor cells. *Oncogene* **19**, 2957-2966.
- Hande, M. P., Samper, E., Lansdorp, P. and Blasco, M. A. (1999). Telomere length dynamics and chromosomal instability in cells derived from telomerase null mice. *J. Cell Biol.* **144**, 589-601.
- Harley, C. B., Futcher, A. B. and Greider, C. W. (1990). Telomeres shorten during ageing of human fibroblasts. *Nature* **345**, 458-460.
- Hemann, M. T., Strong, M. A., Hao, L. Y. and Greider, C. W. (2001). The shortest telomere, not average telomere length, is critical for cell viability and chromosome stability. *Cell* **107**, 67-77.
- Herrera, E., Samper, E., Martín-Caballero, J., Flores, J. M., Lee, H. W. and Blasco M. A. (1999a). Disease states associated to telomerase deficiency appear earlier in mice with short telomeres. *EMBO J.* **18**, 2950-2960.
- Herrera, E., Samper, E. and Blasco, M. A. (1999b). Telomere shortening in mTR^{-/-} embryos is associated with failure to close the neural tube *EMBO J.* **18**, 1172-1181.
- Herrera, E., Martínez-A, C. and Blasco, M. A. (2000). Impaired germinal center reaction in mice with short telomeres. *EMBO J.* **19**, 472-481.
- Johe, K. K., Hazel, T. G., Muller, T., Dugich-Dorjevic, M. M. and McKay, R. D. G. (1996). Single factors direct the differentiation of stem cells from the fetal and adult central nervous system. *Genes Dev.* **10**, 3129-3140.
- Kass-Eisler, A. and Greider, C. W. (2000). Recombination in telomere-length maintenance. *Trends Biochem. Sci.* **25**, 200-204.
- Kim, N. W., Piatyszek, M. A., Prowse, K. R., Harley, C. B., West, M. D., Ho, P. L., Coviello, G. M., Wright, W. E., Weinrich, S. L. and Shay, J. W. (1994). Specific association of human telomerase activity with immortal cells and cancer. *Science* **266**, 2011-2014.
- Klapper, W., Shin, T. and Mattson, M. P. (2001). Differential regulation of telomerase activity and TERT expression during brain development in mice. *J. Neurosci. Res.* **64**, 252-260.
- Lai, K., Kaspar, B. K., Gage, F. H. and Schaffer, D. V. (2003). Sonic hedgehog regulates adult neural progenitor proliferation in vitro and in vivo. *Nat. Neurosci.* **6**, 21-27.
- Langley, E., Pearson, M., Faretta, M., Bauer, U. M., Frye, R. A., Minucci, S., Pelicci, P. G. and Kouzarides, T. (2002). Human SIR2 deacetylates p53 and antagonizes PML/p53-induced cellular senescence. *EMBO J.* **21**, 2383-2396.
- Lee, H. W., Blasco, M. A., Gottlieb, G. J., Horner, J. W., II, Greider, C. W. and DePinho, R. A. (1998). Essential role of mouse telomerase in highly proliferative organs. *Nature* **392**, 569-574.
- Leri, A., Franco, S., Zacheo, A., Barlucchi, L., Chimenti, S., Limana, F., Nadal-Ginard, B., Kajstura, J., Anversa, P. and Blasco, M. A. (2003). Ablation of telomerase and telomere loss leads to cardiac dilatation and heart failure associated with p53 upregulation. *EMBO J.* **22**, 131-139.
- Lois, C. and Alvarez-Buylla, A. (1994). Long-distance neuronal migration in the adult mammalian brain. *Science* **264**, 1145-1148.
- Luo, J., Nikolaev, A. Y., Imai, S., Chen, D., Su, F., Shiloh, A., Guarente, L. and Gu, W. (2001). Negative control of p53 by Sir2alpha promotes cell survival under stress. *Cell* **107**, 137-148.
- Luskin, M. B. (1993). Restricted proliferation and migration of postnatally generated neurons derived from the forebrain subventricular zone. *Neuron* **11**, 173-189.
- Martín-Rivera, L., Herrera, E., Albar, J. P. and Blasco, M. A. (1998). Expression of mouse telomerase catalytic subunit in embryos and adult tissues. *Proc. Natl. Acad. Sci. USA* **95**, 10471-10476.
- McIlraith, J., Bouffler, S. D., Samper, E., Cuthbert, A., Wojcik, A., Szumiel, I., Bryant, P. E., Riches, A. C., Thompson, A., Blasco, M. A. et al. (2001). Telomere length abnormalities in mammalian radiosensitive cells. *Cancer Res.* **61**, 912-915.
- Morrison, S. J., Prowse, K. R., Ho, P. and Weissman, I. L. (1996). Telomerase activity in hematopoietic cells is associated with self-renewal potential. *Immunity* **5**, 201-216.
- Morshead, C. M., Reynolds, B. A., Craig, C. G., McBurney, M. W., Staines, W. A., Morassutti, D., Weiss, S. and van der Kooy, D. (1994). Neural stem cells in the adult mammalian forebrain: a relatively quiescent subpopulation of subependymal cells. *Neuron* **13**, 1071-1082.
- Niida, H., Shinkai, Y., Hande, M. P., Matsumoto, T., Takehara, S., Tachibana, M., Oshimura, M., Lansdorp, P. M. and Furuichi, Y. (2000). Telomere maintenance in telomerase-deficient mouse embryonic stem cells: characterization of an amplified telomeric DNA. *Mol. Cell Biol.* **20**, 4115-4127.
- Ohtsuka, T., Sakamoto, M., Guillemot, F. and Kageyama, R. (2001). Roles of the basic helix-loop-helix genes Hes1 and Hes5 in expansion of neural stem cells of the developing brain. *J. Biol. Chem.* **276**, 30467-30474.
- Ostenfeld, T., Cladwell, M. A., Prowse, K. R., Linskens, M. H., Jauniaux, E. and Svendsen, C. N. (2000). Human neural precursor cells express low levels of telomerase in vitro and show diminishing cell proliferation with extensive axonal outgrowth following transplantation. *Exp. Neurol.* **164**, 215-226.
- Prowse, K. R. and Greider, C. W. (1995). Developmental and tissue-specific regulation of mouse telomerase and telomere length. *Proc. Natl. Acad. Sci. USA* **92**, 4818-4822.
- Reynolds, B. A. and Weiss, S. (1992). Generation of neurons and astrocytes from isolated cells of the adult mammalian central nervous system. *Science* **255**, 1707-1710.
- Rudolph, K. L., Chang, S., Lee, H. W., Blasco, M. A., Gottlieb, G. J., Greider, C. and DePinho, R. A. (1999). Longevity, stress response, and cancer in aging telomerase-deficient mice. *Cell* **96**, 701-712.
- Samper, E., Flores, J. M. and Blasco, M. A. (2001). Restoration of telomerase activity rescues chromosomal instability and premature aging in *Terc*^{-/-} mice with short telomeres. *EMBO Reports* **2**, 800-807.
- Samper, E., Fernández, P., Martín-Rivera, L., Bernad, A., Blasco, M. A. and Aracil, M. (2002). Long-term repopulating ability of telomerase-deficient murine hematopoietic stem cells. *Blood* **99**, 2767-2775.
- Sherr, C. J. and DePinho, R. A. (2000). Cellular senescence: mitotic clock or culture shock? *Cell* **102**, 407-410.
- Shimazaki, T., Shingo, T. and Weiss, S. (2001). The ciliary neurotrophic factor/leukemia inhibitory factor/gp130 receptor complex operates in the maintenance of mammalian forebrain neural stem cells. *J. Neurosci.* **21**, 7642-7653.
- Smith, L. L., Coller, H. A. and Roberts, J. M. (2003). Telomerase modulates expression of growth-controlling genes and enhances cell proliferation. *Nat. Cell Biol.* **5**, 474-479.
- Smogorzewska, A., Karlseder, J., Holtgreve-Grez, H., Jauch, A. and de Lange, T. (2002). DNA ligase IV-dependent NHEJ of deprotected mammalian telomeres in G1 and G2. *Curr. Biol.* **12**, 1635-1644.
- Smogorzewska, A. and de Lange, T. (2002). Different telomere damage signaling pathways in human and mouse cells. *EMBO J.* **21**, 4338-4348.
- Takai, H., Smogorzewska, A. and de Lange, T. (2003). DNA damage foci at dysfunctional telomeres. *Curr. Biol.* **13**, 1549-1556.
- Taupin, P., Ray, J., Fischer, W. H., Suhr, S. T., Hakansson, K., Grubb, A. and Gage, F. H. (2000). FGF-2-responsive neural stem cell proliferation requires CCG, a novel autocrine/paracrine cofactor. *Neuron* **28**, 385-397.
- Temple, S. (2001). The development of neural stem cells. *Nature* **414**, 112-127.
- Thomson, J. A., Itskovitz-Eldor, J., Shapiro, S. S., Waknitz, M. A., Swiergiel, J. J., Marshall, V. S. and Jones, J. M. (1998). Embryonic stem cell lines derived from human blastocysts. *Science* **282**, 1145-1147.
- Tropepe, V., Craig, C. G., Morshead, C. M. and van der Kooy, D. (1997). Transforming growth factor-alpha null and senescent mice show decreased neural progenitor cell proliferation in the forebrain subependyma. *J. Neurosci.* **17**, 7850-7859.
- Vaziri, H., Dragowska, W., Allsopp, R. C., Thomas, T. E., Harley, C. B. and Lansdorp, P. M. (1994). Evidence for a mitotic clock in human hematopoietic stem cells: Loss of telomeric DNA with age. *Proc. Natl. Acad. Sci. USA* **91**, 9857-9860.
- Vaziri, H., Dessain, S. K., Ng Eaton, E., Imai, S. I., Frye, R. A., Pandita, T. K., Guarente, L. and Weinberg, R. A. (2001). hSIR2(SIRT1) functions as an NAD-dependent p53 deacetylase. *Cell* **107**, 149-159.
- Vogelstein, B., Lane, D. and Levine, A. J. (2000). Surfing the p53 network. *Nature* **408**, 307-310.
- Wong, K. K., Maser, R. S., Bachoo, R. M., Menon, J., Carrasco, D. R., Gu, Y., Alt, F. W. and DePinho, R. A. (2003). Telomere dysfunction and Atm deficiency compromises organ homeostasis and accelerates ageing. *Nature* **421**, 643-648.
- Xu, D., Wilson, T. J., Chan, D., De Luca, E., Zhou, J., Hertzog, P. J. and Kola, I. (2002). Ets1 is required for p53 transcriptional activity in UV-induced apoptosis in embryonic stem cells. *EMBO J.* **21**, 4081-4093.